Synthesis and Characterization of a Three-dimensional Porous Compound: $[Cu(H_2O)_6][\{Cu(H_2O)_2\}_2\{Cu(H_2O)_4H_4W_{12}O_{42}\}] \cdot 12H_2O$

Chun-jing Zhang, Ya-guang Chen, Dong-mei Shi, and Hai-jun Pang

Key Laboratory of Polyoxometalate Science of Ministry of Education, College of Chemistry,
Northeast Normal University, Changchun 130024, P. R. China

Reprint requests to Dr. Yaguang Chen. E-mail: chenyg146@nenu.edu.cn

Z. Naturforsch. **2008**, *63b,* 187 – 192; received September 28, 2007

A novel transition metal polyoxotungstate, $[Cu(H_2O)_6][\{Cu(H_2O)_2\}_2\{Cu(H_2O)_4H_4W_{12}O_{42}\}] \cdot 12H_2O$ (**1**), has been synthesized in aqueous solution and characterized by single-crystal X-ray diffraction, elemental analysis, IR and UV/vis spectroscopy, and TG analysis. The paradodecatungstate anions $[H_2W_{12}O_{42}]^{10-}$ are linked by CuO_6 octahedra, forming a three-dimensional (3D) structure. The magnetic susceptibility of compound **1** in the temperature range 2 – 300 K shows the presence of antiferromagnetic interactions within the uniform Cu2···Cu3 chains.

Key words: Polyoxometalates, Transition Metal Bridge, 3D Architecture, Magnetic Properties

Introduction

Owing to the special features of transition metal oxide surfaces and the role of polyoxometalate (POM) clusters in several areas of current interest [1], research on chemically robust POM-based composite materials is highly attractive. It is especially fascinating when POM clusters are employed as building blocks to construct extended solid frameworks.

Up to now, one of the challenging tasks in POMs chemistry is to design and synthesize multidimensional porous metal-organic frameworks [2 – 7]. In comparison with many inorganic-organic hybrid materials with extended frameworks based on POMs, generating true metal oxide surfaces and framework materials without the incorporation of additional conventional ligands holds a large potential [8]. This kind of material is usually stable and insoluble in common organic solvents. This property is very advantageous to expand the application of POM-based materials in chemically bulk-modified electrodes [9].

The paradodecatungstate anion $[H_2W_{12}O_{42}]^{10-}$ with its particular structural features, sufficient charge density and multiple coordination sites, provides numerous possibilities of intermolecular linkages according to the linking rules of selected building blocks [1a, 10 – 12]. On the other hand, transition metal ions with multiple coordination requirements, oxophilicity, unique catalytic and magnetic properties, have been used in developing POMs incorporating transition metals. Here, we report the synthesis and characterization of a unique 3D, purely inorganic, porous compound formed by paradodecatungstate and first-row transition metal cations in a facile synthetic method.

Results and Discussion

Synthesis

Compound **1** was obtained from a mixture of $(NH_4)_6[H_2W_{12}O_{40}] \cdot 3H_2O$ and $Cu(CH_3COO)_2 \cdot 2H_2O$. It was an unexpected product during our attempt to synthesize compounds based on the $[H_2W_{12}O_{40}]^{6-}$ cluster. Although the formation mechanism is not very clear, we propose the following steps: (i) Disassembly-reconstitution of the polyoxoanion: the reaction equilibrium of polyoxometalate chemistry in aqueous solution is multifold, so subtle changes of pH, temperature or time play an important role in the reaction. Under the conditions we chose (initial pH = 3.85, 80 °C, 1 h and in presence of Cu^{2+} ions), the $[H_2W_{12}O_{40}]^{6-}$ clusters first decomposed to triangular W_3O_{10} groups and some of those groups rearranged into belt-type W_3O_{11} groups. Subsequently, the two types of groups became tied together through interconnecting corners, forming a new cluster $[H_2W_{12}O_{42}]^{10-}$; (ii) structural feature of the polyoxoanion: additional terminal oxygen atoms in the W_3O_{11} groups are prone to link metal cations [13] which make the whole compound stable. The pH of

0932–0776 / 08 / 0200–0187 $ 06.00

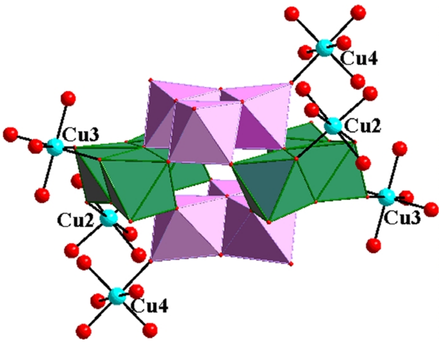

Fig. 1. Representation of the molecular structure of **1**. The hydrogen atoms and crystal water molecules are omitted for clarity.

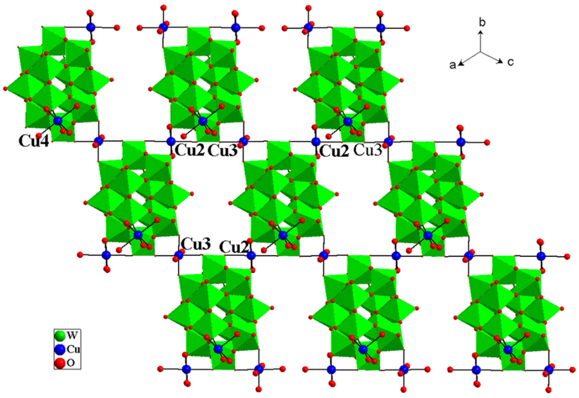

Fig. 2. The 2D layer along the [1 1 1] plane.

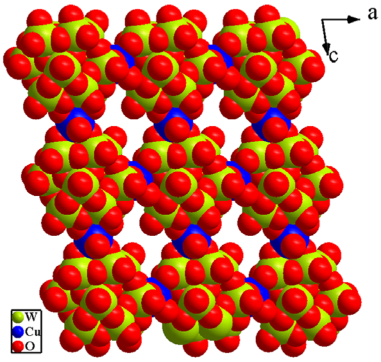

Fig. 3. Space-filling representation of the pore structure.

the reaction mixtures seems to be crucial because the solid is isolated only in a narrow pH region (3.5 – 4.1).

Crystal structure of the compound

The title compound consists of $[\{Cu(H_2O)_2\}_2\{Cu(H_2O)_4H_4W_{12}O_{42}\}]^{2-}$ anions, discrete $[Cu(H_2O)_6]^{2+}$ cations and H_2O molecules of crystallization. The paratungstate-B unit $[H_2W_{12}O_{42}]^{10-}$ illustrated in Fig. 1 is structurally identical to those reported previously, *e. g.* in $K_6[Co(H_2O)_4]_2[H_2W_{12}O_{42}] \cdot 14H_2O$ [14], $(NH_4)_7[Bi(H_2W_{12}O_{42})] \cdot 20H_2O$ [15], and $H_2\{[K(H_2O)_2]_2[Ln(H_2O)_5]_2(H_2M_{12}O_{42})\} \cdot nH_2O$ [16]. This polyoxoanion is centrosymmetric and consists of four corner-sharing groups of two types, cap-type and belt-type, and each group contains three edge-sharing WO_6 octahedra. All tungsten atoms exhibit a +VI oxidation state as confirmed by bond valence sum calculations [17], and possess distorted octahedral coordination. The $[H_2W_{12}O_{42}]^{10-}$ cluster acts as a decadentate ligand coordinating to six copper(II) ions through the terminal oxygen atoms (see Fig. 1), such that each $[H_2W_{12}O_{42}]^{10-}$ cluster is connected to six CuO_6 octahedra.

As to the metallic atoms in compound **1**, there are four crystallographically unique copper centers with different coordination environments. The Cu1 atom is in the centre of an octahedron defined by six water molecules with Cu1–O bond lengths in the range from 1.912(15) to 2.389(14) Å in a discrete cation. The Cu2 octahedra are formed by four oxygen atoms which belong to the belt-type W_3O_{11} groups coming from two paratungstate cores and two H_2O molecules with Cu2–O bond lengths in the range from 1.943(10) to 2.550(11) Å. The Cu3 octahedra are formed similarly to those of Cu2 with the Cu3–O bond lengths in the range from 1.969(11) to 2.385(11) Å. The Cu4 atom is coordinated by two terminal oxygen atoms of the cap-type of two $[H_2W_{12}O_{42}]^{10-}$ clusters and four H_2O molecules with Cu4–O bond lengths in the range from 1.904(12) to 2.380(12) Å. All these bond lengths are within the normal ranges and in close agreement with those described in the literature [18].

It should be noted that two terminal oxygen atoms linking Cu2 and Cu3 come from the same WO_6 octahedra where two *cis* terminal oxygen atoms make it easier to link metal ions [13]. Such a structure is suitable to build high-dimensional architectures. As shown in Fig. 2, neighboring $[H_2W_{12}O_{42}]^{10-}$ clusters are connected by $[Cu2(H_2O)_2]^{2+}$ and $[Cu3(H_2O)_2]^{2+}$ cations forming a square belt (POMs-Cu2-POMs-Cu3-POMs-Cu2-POMs-Cu3) in the [1 1 1] plane. The infinite repetitions of the square belt gives 2D layers (Fig. 2). These layers are further connected by Cu4 forming a 3D structure with two tunnels with a dumbbell cross section (Fig. 3). Discrete $[Cu(H_2O)_6]^{2+}$ cations are located in the channels along the *b* axis. Viewed along the *a* axis extensive hydrogen bonds can be

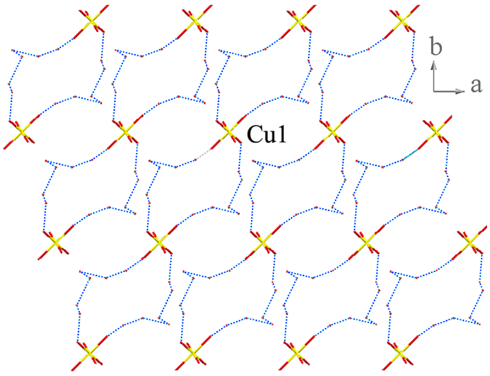

Fig. 4. Hydrogen bonds in crystals of the complex viewed along the *c* axis.

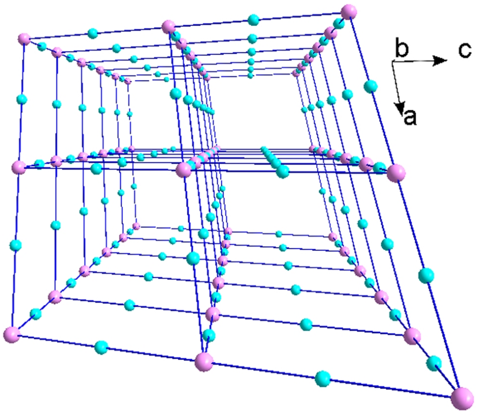

Fig. 5. Simplified schematic representation of the 3D open-framework structure.

clearly observed between the H_2O molecules of crystallization as well as the $[Cu(H_2O)_6]^{2+}$ cations with O···O interatomic lengths between 2.732 and 3.007 Å (Fig. 4). Furthermore, the oxygen atoms of the polyoxotungstate units also form hydrogen bonds with H_2O molecules, which make the crystal structure of **1** more stable.

By reducing multidimensional structures to simple node-and-connector reference nets, the crystal structure is reduced to an irreducible net resulting from the combination of six-connecting nodes with an $(8^{12}12^{3})$ topology: the polyoxometalate clusters are simplified as nodes, and the Cu–O bonds are represented as the edges, as show in Fig. 5.

UV/vis spectrum

The electronic spectrum of compound **1** in aqueous solution (Fig. 6) displays an absorption peak at 252 nm which is attributed to the $d\pi$–$p\pi$ charge transfer absorption band of the W=O bond. The weak absorption in the visible region at 779 nm may be assigned to *d–d* transitions of Cu^{2+} cations in a distorted octahedral environment.

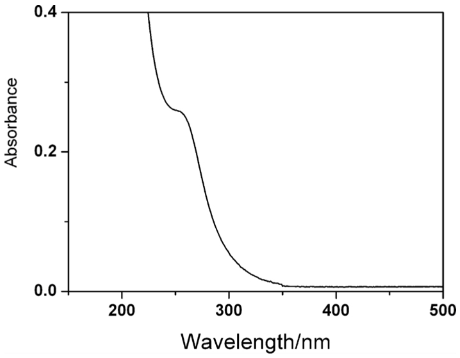

Fig. 6. UV/vis spectrum of the complex.

Thermal analysis

The weight loss of compound **1** in the temperature range of 0 – 700 °C corresponds to the release of all water molecules. The weight loss of 5.17 % at 45 – 110 °C is attributed to the loss of crystal water (calcd. 5.99 %). In the ranges 110 – 213 and 213 – 413 °C, the weight losses are 2.72 and 4.16 %, respectively, in agreement with the removal of 6 H_2O molecules coming from the $[Cu(H_2O)_6]^{2+}$ cations and 8 H_2O molecules from the $[\{Cu(H_2O)_2\}_2\{Cu(H_2O)_4H_4W_{12}O_{42}\}]^{2-}$ anions, respectively (calcd. 2.99 % for the former; 3.99 % for the latter). The small weight loss of 0.97 % between 413 and 700 °C is consistent with the release of two H_2O molecules (calcd. 1 %), according to the decomposition reaction, $Cu_4[H_2W_{12}O_{42}] \rightarrow 4CuO \cdot 12WO_3 + 2H_2O$. The total weight loss of 13.59 % agrees with the calculated value of 13.99 %.

Magnetic properties

The variable-temperature magnetic susceptibilities of newly prepared compound **1** were measured from 2 to 300 K at a fixed field strength of 1000 Oe. The result is shown in the form of a $\chi_m T$ *vs.* T curve. The $1/\chi_m$ *vs.* T curve of **1** is also given in the inset (Fig. 7). When the sample is cooled from r. t., $\chi_m T$ decreases smoothly from 1.72 (300 K) to 1.28 emu · K · mol^{-1} (2 K). The inverse susceptibility ($1/\chi_m$) plot as a function of temperature (T) is almost linear in the range of 100 – 300 K, closely following the Curie-Weiss law,

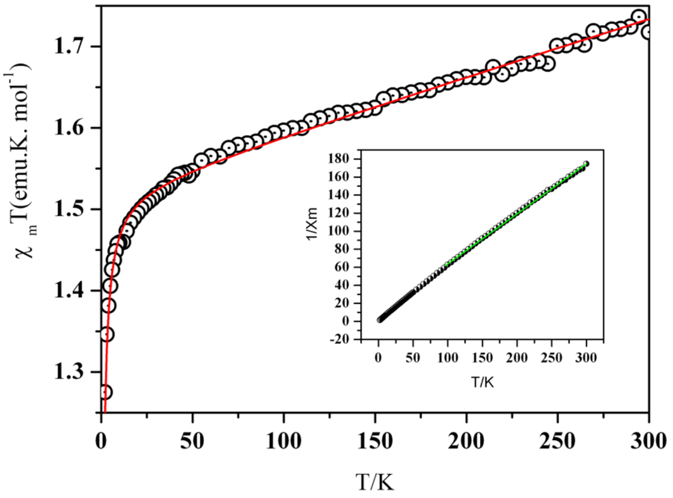

Fig. 7. The temperature dependence of the reciprocal magnetic susceptibility $1/\chi_m$ and the product χ_m T for compound **1**.

giving a Curie constant C = 1.79 cm^3 K mol^{-1} and a Weiss constant θ (-12.9 K) < 0, suggesting the occurrence of antiferromagnetic exchange interactions in the title compound.

At r.t., the effective magnetic moment (μ_{eff}) determined from the equation μ_{eff} = 2.828 $(\chi_m T)^{1/2}$ is 3.71 μ_B, which is obviously smaller than the expected spin-only value (4.89 μ_B) for four isolated Cu^{2+} atoms (S = 2; g = 2.00). The result may be explained as follows: as illustrated in the structure description, the Cu1 atoms exist in discrete cations. The antiferromagnetic exchange interactions therefore can only exist between WO_6 group-bridged Cu2···Cu3 chains, because the Cu4 atoms are also separated far from other Cu^{2+}cations by WO_6 units (Fig. 2). The singlet-triplet energy gap (J) is defined by the Hamiltonian $H = -JS_AS_B$ ($S_A = S_B$ = 1/2), and the susceptibility can be described by the following formula based on a modified uniform chain model [19]:

$$\chi_{chain} = N\beta^2 g^2 S(S+1)(1+u)/(1-u)/3kT \quad (1)$$

where $u = \coth[JS(S+1)/kT] - kT/JS(S+1)$

$$\chi_m = (1-\rho)\chi_{chain} + 2\rho(N\beta^2 g^2/3kT)S(S+1) \quad (2)$$

$$\chi_M = \chi_m/[1-\chi_m(2zJ'/N\beta^2 g^2)] \quad (3)$$

Using this model, the susceptibility was simulated, giving the best fit with parameters $J = -0.05$ cm^{-1} and g = 1.43. The small J value might be attributed to the WO_6 group-bridged linkages, which have an unfavorable effect on the magnetic interaction. So the effective magnetic moment should be 3.5 μ_B (g = 1.43). The result supports the occurrence of Cu2···Cu3 coupling through a tungstate bridge.

Conclusions

In summary, we have obtained and structurally characterized $[Cu(H_2O)_6][\{Cu(H_2O)_2\}_2\{Cu(H_2O)_4H_4W_{12}O_{42}\}] \cdot 12H_2O$ for the first time. The synthesis of compound **1** from the components indicates the diversity of pathways for attaining novel structures and species. The magnetic behavior of **1** reveals the interactions between the copper(II) cations. It appears that the paratungstate-B cluster is a good candidate for synthesizing new compound with varying architectures and properties, because of its sufficient charge density at the surface oxygen atoms and other structural features.

Experimental Section

General procedures

All reagents were commercially available and were used without further purification. $(NH_4)_6[H_2W_{12}O_{40}] \cdot 3H_2O$ was synthesized according to the literature [20] and characterized by IR and UV/vis spectroscopy, and TG analysis. Elemental analyses (Cu, W) were carried out with a Leaman inductively coupled plasma (ICP) spectrometer. IR spectra on KBr pellets were recorded on a Nicolet 170SX FT-IR spectrophotometer in the range 4000 – 400 cm^{-1}. The UV/vis spectra were recorded in the range of 200 – 1200 nm in aqueous solution on a DU-70 spectrophotometer. TG analysis was recorded with a Netzsch STA 449C microanalyzer in an atmosphere of nitrogen at a heating rate of 10 °C min^{-1}. Variable temperature magnetic susceptibility measurements were

Table 1. Crystal data and structure refinement for **1**.

Empirical formula	$H_{52}Cu_4O_{68}W_{12}$
M_r	3600.70
Color, habit	blue, block
Cryst. size, mm^3	$0.11 \times 0.11 \times 0.11$
Crystal system; space group	triclinic; $P\bar{1}$ (no. 2)
a, Å	10.6551(5)
b, Å	12.7418(6)
c, Å	13.2833(6)
α, deg	63.177(1)
β, deg	72.521(1)
γ, deg	67.389(1)
V Å^3	1468.0(11)
Z	1
D_{calcd}, g cm^{-3}	4.07
$\mu(\text{Mo}K_\alpha)$, cm^{-1}	24.9
$F(000)$, e	1600
hkl Range	$-13 \le h \le 14$, $-7 \le k \le 17$, $-17 \le l \le 17$
Absorption correction	none
Refl. measured/unique	9206/7318
R_{int}	0.033
Data/restraints/parameters	6736/0/380
GoF (F^2)	0.983
$R_1/wR_2[I > 2\sigma(I)]$	0.047/0.106
R_1/wR_2 (all data)	0.071/0.125
$\Delta\rho_{\text{fin}}$ (max/min), e Å^{-3}	1.96/−3.68

carried out on a Quantum Design MPMS-5SQUID magnetometer with an applied field of 1000 Oe. Diamagnetic correction was estimated from Pascal's constants.

Synthesis of $[Cu(H_2O)_6][\{Cu(H_2O)_2\}_2\{CuH_2O)_4H_4W_{12}O_{42}\}] \cdot 12H_2O$ *(**1**)*

In a typical experiment, $(NH_4)_6[H_2W_{12}O_{40}] \cdot 3H_2O$ (3.008 g, 1 mmol) was first suspended in distilled water (10 mL), to which a solution of $Cu(CH_3COO)_2 \cdot 2H_2O$ (0.399 g, 1 mmol) was added dropwise with stirring. The initial pH of the mixture was adjusted to 3.85. The mixture was heated for 1 h at 80 °C and allowed to cool to r. t. Then a minor precipitate was filtered off. The filtrate was left to evaporate slowly under ambient conditions. After five days, light blue block-shaped crystals were isolated in about 40 % yield (based on Cu). – $[Cu(H_2O)_6][\{Cu(H_2O)_2\}_2\{Cu(H_2O)_4H_4W_{12}O_{42}\}] \cdot 12H_2O$: calcd. Cu 7.06, W 61.27; found Cu 6.96, W 61.09. – IR (KBr): ν = 3434 (vs), 1622 (s), 940 (s), 860 (m), 723 (m), 567 (w), 493 (m), 409 (m) cm^{-1}.

Table 2. Selected bond lengths (Å) for compound **1**[a].

Cu(1)–O(4W)$^{\#2}$	1.912(15)	Cu(1)–O(4W)	1.912(15)
Cu(1)–O(5W)$^{\#2}$	1.939(15)	Cu(1)–O(5W)	1.939(15)
Cu(1)–O(6W)$^{\#2}$	2.389(14)	Cu(1)–O(6W)	2.389(14)
Cu(2)–O(8)$^{\#3}$	1.943(10)	Cu(2)–O(8)	1.943(10)
Cu(2)–O(1)$^{\#3}$	2.551(11)	Cu(2)–O(8)	2.551(11)
Cu(2)–O(13W)	1.993(11)	Cu(2)–O(13W)$^{\#3}$	1.993(11)
Cu(3)–O(20)$^{\#4}$	1.976(10)	Cu(3)–O(20)	1.976(10)
Cu(3)–O(10W)$^{\#4}$	1.969(11)	Cu(3)–O(10W)	1.969(11)
Cu(3)–O(15)$^{\#4}$	2.385(11)	Cu(3)–O(15)	2.385(11)
Cu(4)–O(12W)	1.904(12)	Cu(4)–O(12W)$^{\#5}$	1.904(12)
Cu(4)–O(21)$^{\#5}$	1.967(10)	Cu(4)–O(21)	1.967(10)
Cu(4)–O(9W)$^{\#5}$	2.380(12)	Cu(4)–O(9W)	2.380(12)

[a] Symmetry transformations used to generate equivalent atoms: $^{\#2}$ $-x+2, -y-2, -z+1$; $^{\#3}$ $-x+4, -y-2, -z$; $^{\#4}$ $-x+3, -y-2, -z+1$; $^{\#5}$ $-x+3, -y, -z$.

X-Ray crystallography

X-ray diffraction data were collected on a SMART CCD diffractometer with graphite monochromated MoK_α radiation at r. t. The structure was solved by Direct Methods and refined by full-matrix least-squares on F^2 with the SHELX-97 program package [21]. The non-hydrogen atoms were located with difference Fourier syntheses, and the hydrogen atoms were generated geometrically. For **1**, a total of 9206 reflections ($1.87 \le \theta \le 28.3°$) were collected with 7318 unique ones (R_{int} = 0.033), of which 6736 reflections with $I \ge 2\sigma(I)$ were used for the structure refinement. The crystallographic data for **1** are listed in Table 1, and selected bond lengths are presented in Table 2.

Further details of the crystal structure investigation may be obtained from Fachinformationszentrum Karlsruhe, 76344 Eggenstein-Leopoldshafen, Germany (fax: +49-7247-808-666; e-mail: crysdata@fiz-karlsruhe.de, http://www.fiz-informationsdienste.de/en/DB/icsd/depot_anforderung.html) on quoting the deposition number CSD-418106.

Acknowledgement

This work was supported by the Analysis and Testing Foundation of the Northeast Normal University.

[1] a) M. T. Pope, *Heteropoly and Isopoly Oxometalates*, Springer, Berlin, **1983**; b) M.T. Pope, A. Müller, *Angew. Chem.* **1991**, *103*, 56; *Angew. Chem. Int. Ed.*. **1991**, *30*, 34; c) C.L. Hill, *Chem. Rev.* **1998**, *98*, 1; d) I.V. Kozhevnikov, *Chem. Rev.* **1998**, *98*, 171; e) T. Yamase, *Chem. Rev.* **1998**, *98*, 307; f) A. Müller, F. Peters, M.T. Pope, D. Gatteschil, *Chem. Rev.* **1998**, *98*, 239.

[2] H. Li, M. Eddaoudi, M. O'Keeffe, O.M. Yaghi, *Nature* **1999**, *402*, 276.

[3] S. S.-Y. Chui, S. M.-F. Lo, J. P. H. Charmant, A. G. Orpen, I. D. Williams, *Science* **1999**, *283*, 1148.

[4] B. Chen, M. Eddaoudi, S. T. Hyde, M. O'Keeffe, O. M. Yaghi, *Science* **2001**, *291*, 1021.

[5] M. Eddaoudi, J. Kim, N. Rosi, D. Vodak, D.V. Wachter, M. O'Keeffe, O.M. Yaghi, *Science* **2002**, *295*, 469.

[6] N. L. Rosi, J. Eckert, M. Eddaoudi, D. T. Vodak, J. Kim, M. O'Keeffe, O. M. Yaghi, *Science* **2003**, *300*, 1127.

[7] S. L. James, *Chem. Soc. Rev.* **2003**, *32*, 276.

[8] a) M. I. Khan, E. Yohannes, D. Powell, *Chem. Commun.* **1999**, *1*, 23; b) M. I. Khan, E. Yohannes, R. Doedens, *Angew. Chem.* **1999**, *111*, 1374; *Angew. Chem. Int. Ed.* **1999**, *38*, 1292; c) X. B. Cui, J. Q. Xu, H. Meng, S. T. Zheng, G. Y. Yang, *Inorg. Chem.* **2004**, *43*, 8005.

[9] a) K. Kalcher, *Electroanalysis* **1990**, *2*, 419; b) X. L. Wang, E. B. Wang, Y. Lan, C. W. Hu, *Electroanalysis* **2002**, *14*, 1116.

[10] H. T. Evans Jr., E. Prince, *J. Am. Chem. Soc.* **1983**, *105*, 4838.

[11] C. Gimenez-Saiz, J. R. Galan-Mascaros, S. Triki, E. Coronado, L. Ouahab, *Inorg. Chem.* **1995**, *34*, 524.

[12] I. Loose, M. Bösing, R. Klein, B. Krebs, R. P. Schulz, B. Scharbert, *Inorg. Chim. Acta* **1997**, *263*, 99.

[13] Y. G. Chen, L. K. Yan, X. R. Hao, K. Liu, X. H. Wang, P. P. Lu, *Inorg. Chim. Acta* **2006**, *359*, 2550.

[14] C. Gimenez-Saiz, J. R. Galan-Mascaros, S. Triki, E. Coronado, L. Ouahab, *Inorg. Chem.* **1995**, *34*, 524.

[15] Z. H. Xu, X. L. Wang, Y. G. Li, E. B. Wang, C. Qin, Y. L. Si, *Inorg. Chem. Commun.* **2007**, *10*, 276.

[16] X. T. Zhang, D. Q. Wang, J. M. Dou, S. S. Yan, X. X. Yao, J. Z. Jiang, *Inorg. Chem.* **2006**, *45*, 10629.

[17] I. D. Brown, D. Altermatt, *Acta Crystallogr.* **1985**, *B41*, 244.

[18] H. Y. An, E. B. Wang, D. R. Xiao, Y. G. Li, Z. M. Su, L. Xu, *Angew. Chem.* **2006**, *118*, 918; *Angew. Chem. Int. Ed.* **2006**, *45*, 904.

[19] H. Z. Kou, B. C. Zhou, D. Z. Liao, R. J. Wang, Y. D. Li, *Inorg. Chem.* **2002**, *41*, 6887.

[20] J. H. Son, Y. U. Kwon, O. H. Han, *Inorg. Chem.* **2003**, *42*, 4153.

[21] G. M. Sheldrick, SHELXS/L-97, Programs for Crystal Structure Determination, University of Göttingen, Göttingen (Germany) **1997**.